7.
Seismic Retrofitting of Rectangular Bridge Columns with Composite Straps

H. Saadatmanesh, M.R. Ehsani, M.EERI, and L. Jin

Behavior of typical rectangular bridge columns with substandard design details for seismic forces was investigated. The poor performance of this type of column attested to the need for effective and economical seismic upgrading techniques. A method utilizing fiber reinforced polymer (FRP) composites to retrofit existing bridge columns is investigated in this paper. High-strength FRP straps are wrapped around the column in the potential plastic hinge region to increase confinement and to improve the behavior under seismic forces. Five rectangular columns with different reinforcement details were constructed and tested under reversed cyclic loading. Two columns were not retrofitted and were used as control specimens so that their hysteresis response could be compared with those for retrofitted columns. The results of this study indicated that significant improvement in ductility and energy absorption capacity can be achieved as a result of this retrofitting technique.

INTRODUCTION

During the last three decades, there has been a great deal of research on the behavior of structures subjected to earthquake forces. These activities have resulted in the development of sophisticated methodologies and procedures for the design of earthquake-resistant structures. However, there still exist a very large number of buildings and bridges that were designed prior to the development of modern seismic design guidelines that require retrofit. These structures present significant risk to the safety of the public in the event of an earthquake as evidenced by the recent earthquakes in Japan and California. A major cause of the failure of bridge columns in these earthquakes was the lack of adequate transverse reinforcement and poor starter-bar details in the columns.

In this paper, the results of an investigation on seismic strengthening of rectangular concrete columns using high-strength fiber reinforced plastic (FRP) composite straps are discussed. The procedure involves wrapping layers of thin, flexible straps or tapes of resin-impregnated fiber composites around the column in the potential plastic hinge zone or along the entire height of the column if desired, as shown in Figure 1. An epoxy resin is brushed on to the strap while wrapping

(HS, MRE) Department of Civil Engineering and Engineering Mechanics, University of Arizona. Bldg. #72, Room 206, Tucson, Arizona, 85721.
(LJ) Graduate Research Assistant, Department of Civil Engineering and Engineering Mechanics, University of Arizona, Bldg. #72, Room 206, Tucson, 85721

for interlaminar bonding of the layers of the strap. The composite strap wrapped around the column in this manner, will provide external confinement, prevent crushing and spalling of the concrete shell, and prevent buckling of the longitudinal reinforcement. To further enhance the confinement, lateral pressure can be induced on to the column by the use of expansive grout, or by pressure injecting epoxy resin in the gap between the composite strap and the column face (active retrofit). Such gaps can be produced by placing spacers between the composite strap and the column during the wrapping operation.

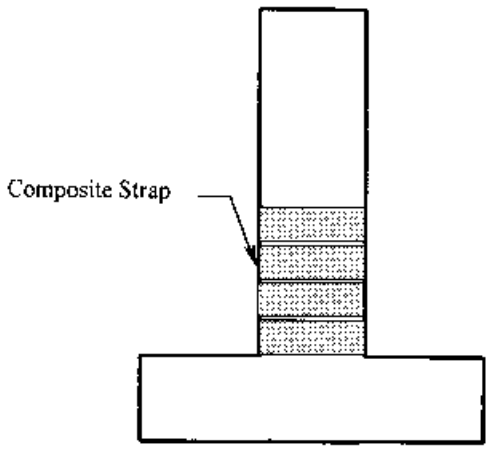

Figure 1. Typical concrete column wrapped with composite strap in the potential plastic hinge region.

A total of five 1/5-scale rectangular columns were cast and tested under reversed cyclic loading. The basic design variables in these specimens were the reinforcement details, i.e., lapped starter bars vs. continuous rebars and shape of the cross section, i.e., rectangular vs. oval shaped. Two columns were not retrofitted and were used as control specimens. A comparison of responses of retrofitted and unretrofitted columns indicated significant improvement in ductility and energy absorption capacity as a result of retrofitting with composite straps.

PREVIOUS WORK

Major seismic retrofit programs for bridge structures have been initiated in the United States, New Zealand and Japan since the early 1970's. Many techniques that have been utilized in the retrofit design process have been based mainly on experimental testing of scaled down models of structural elements within the bridge structures.

To verify the seismic retrofit for upgrading portions of the San Francisco double-deck viaducts for standards of seismic performance equal to or higher than those expected of new bridges, a half-scale model of a typical section of the double-deck viaduct was successfully tested under simulated seismic forces and displacement at the University of California, San Diego (Priestly, et al., 1993).

Oval steel jackets were used for retrofitting rectangular reinforced concrete bridge columns (Sun, et al., 1992; Priestly, et al., 1988). A total of six column specimens were constructed with a 40 percent dimensional scale factor. The columns were tested in the strong direction as well as the weak direction. The oval steel jacket was effective for retrofitting rectangular concrete bridge columns, since the retrofit system was able to transfer effective membrane confining pressure to the core and cover concrete to increase the strength and ductility, and to provide clamping action to lapped starter bars in the columns to enhance bond strength. Test results showed that columns retrofitted with oval steel jacket exhibited stable and ductile lateral response up to displacement ductility level of 7. It was noted, however, that the columns with high longitudinal steel ratio failed in shear at the column sections above the steel jacket.

An investigation on seismic strengthening of concrete columns with carbon fiber composites was conducted in Japan (Kasumata, et al., 1988). Ten 1/4-scale column specimens with square cross sections of 200 x 200 mm (7.87 in. x 7.87 in.) were tested. Because the stress transfer between the carbon fibers and concrete occurred mainly at the corners due to the rectangular geometry of the cross section, four corners were beveled and rounded to reduce stress concentration in the carbon fibers. To show the effectiveness of the interface between the carbon fibers and concrete, two sets of specimens were studied. For the first set, isolating film was provided between the fiber and the concrete; for the other set, the fibers were epoxy bonded directly on to the concrete substrate. The test results showed that wrapping of carbon fibers around the column greatly increased the earthquake-resistant capacity of the columns. In particular, the following conclusions were drawn: (1) ultimate displacement and energy dissipation were increased approximately linearly with the quantity of carbon fibers used; (2) the earthquake-resistant capacity of columns retrofitted with carbon fibers could be correlated roughly with the original reinforced concrete column having only hoop reinforcement; (3) the quantity of carbon fiber and steel hoop reinforcement were mutually convertible when an effective strength ratio was introduced; and (4) when the quantity of carbon fiber was the same, there was no noticeable difference in ultimate displacement between the specimens with isolating film and those without the isolating film.

FIBER COMPOSITES

Fiber composite materials generally possess higher strength to weight ratio than conventional materials. Among other advantages of fiber composites are their corrosion resistance, versatility, and light weight. They are made of small fibers such as glass, carbon, kevlar, etc., placed in a resin matrix. The primary load carrying element within a composite is the fiber. The fiber has a strong influence on the mechanical properties of the composite such as strength and elastic modulus. The resin provides a mechanism for the transfer of load among the fibers. It also protects the fibers from abrasion and other environmental and chemical attacks. The fibers within the composite can be oriented in a single direction (unidirectional) or several directions to optimize the structural performance. Unidirectional composites usually have a linear stress-strain relationship to failure.

E-glass, by far, is the most common type of fiber used in polymer composites due to its high-strength and low cost. In this study, 152 mm (6 in.) wide unidirectional E-glass tapes were used

in the construction of composite straps. The fabrication of the composite straps involved laying the E-glass tape and saturating it with polyester resin. A layer of mylar sheet was then placed on the wet tape, the two were then rolled around a mandrel representing the size and shape of the column cross section and placed in an oven to cure. The mylar sheet was provided to prevent bonding of the composite tape to itself while curing. The wet composite tape was cured at 160°F for forty minutes. Due to the small thickness, the cured strap was flexible enough to be wrapped around both oval and rectangular columns (Fig. 2).

The stress-strain relationship of the E-glass composite straps with three different fiber volume ratios are shown in Figure 3, where V_f – fiber volume ratio, is defined as the volume of the fibers divided by the total volume of the composite. As can be seen from this figure, the strength and modulus of the strap changes considerably with the amount of fiber. The strap with $V_f = 50.2\%$ was relatively easy to produce in the laboratory and therefore was used for retrofitting of the columns in this study. The lower strength of this type of strap can be compensated for by higher number of layers to achieve a desired hoop strength.

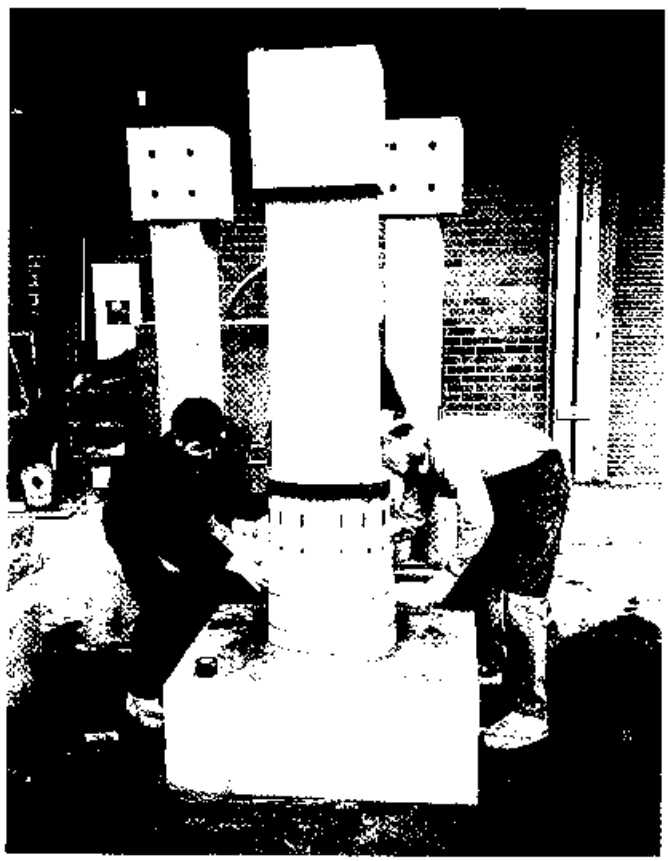

Figure 2. Column being wrapped with composite strap.

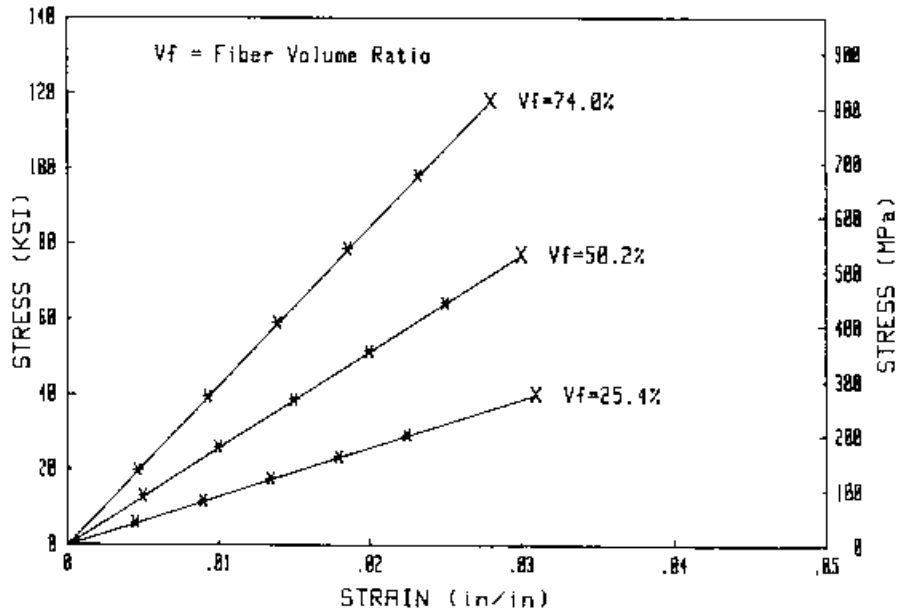

Figure 3. Typical stress-strain curves of composite strap.

TEST SPECIMENS

Five rectangular, reinforced concrete bridge column footing assemblages were designed with a scale factor 1/5 that of the prototype bridge columns. The test specimens were designed to model typical pre-1971 design of existing highway bridge columns in a zone of high seismic risk. Each specimen modeled a prototype single column bent to emphasize two problems: (1) inadequate starter bar lap length; (2) insufficient transverse reinforcement, as shown in Figure 4. The composite strap was applied only in the potential plastic hinge region estimated to be twice that of the effective depth of the cross section; i.e., in the 635 mm (25 in.) long portion of the column above the top face of the footing. Two types of strap configurations were designed and fabricated in the laboratory, as shown in Figure 5. In addition to rectangular strap configuration, an oval shape (Figure 5b) was used to examine the effectiveness of the confining action of these two configurations. Figure 6 shows a typical column with its cross section modified into an oval shape using fast curing cement and then wrapped with the composite straps in the plastic hinge region. The strap for the oval-shaped column did not need to be prefabricated in the form of an "oval," since the cross section did not contain sharp corners and the strap was flexible enough to be easily wrapped around the section. The behavior of the columns with these strap configurations will be discussed in subsequent sections.

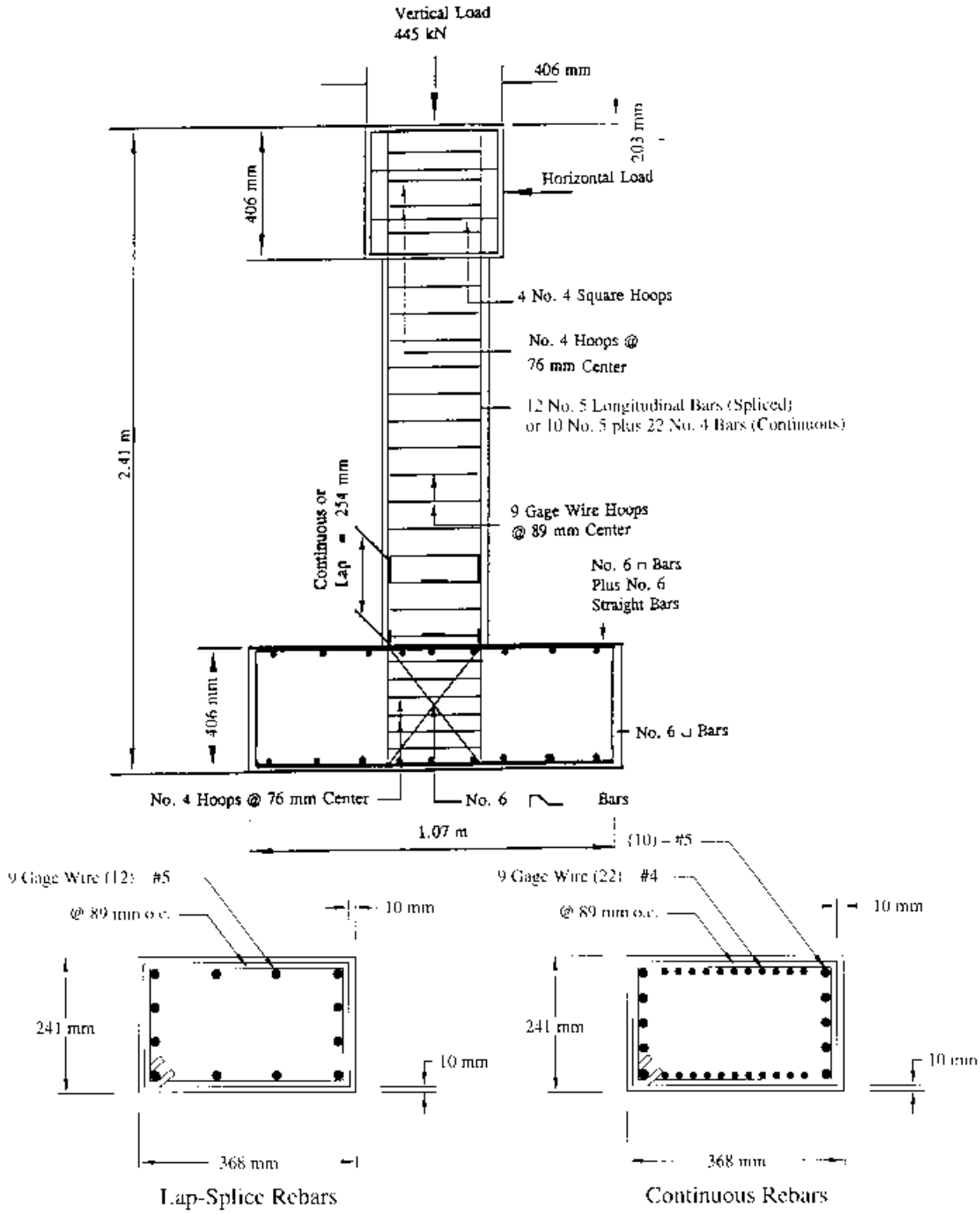

Figure 4. Reinforcement details of column specimens.

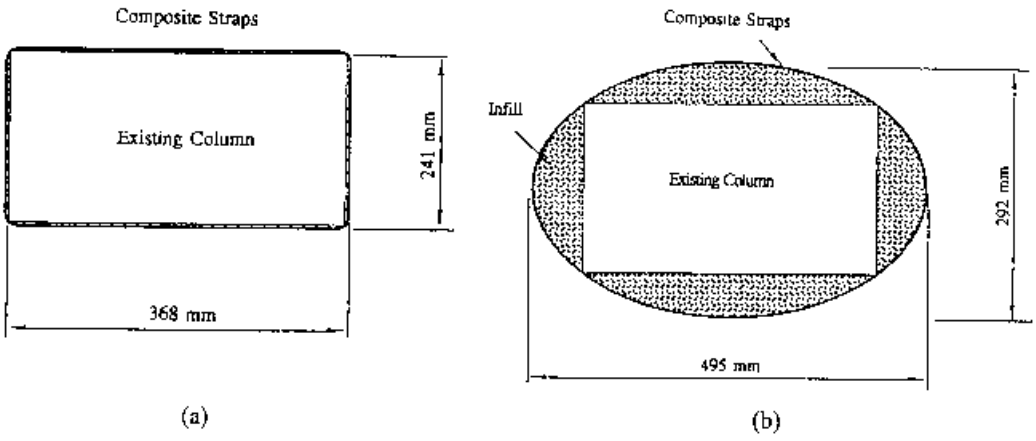

Figure 5. Retrofit with (a) Rectangular and (b) Oval-Shaped composite straps.

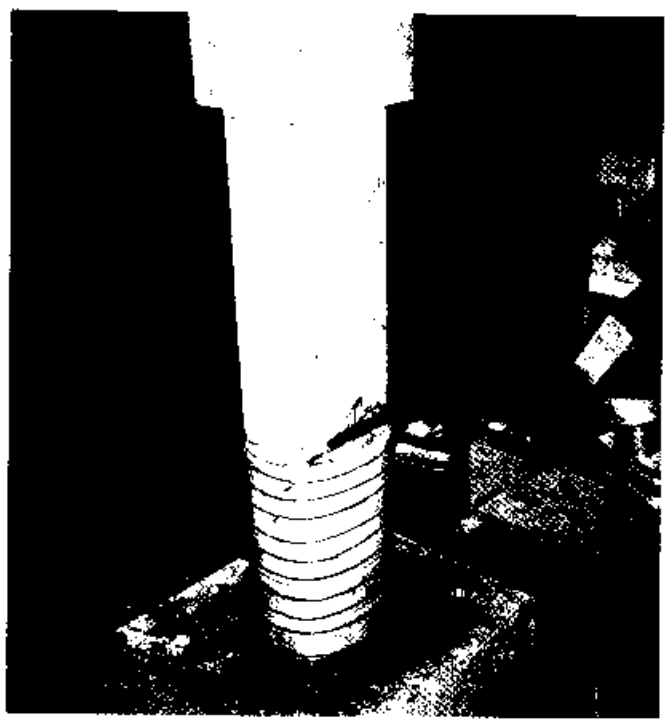

Figure 6. Rectangular column modified into an oval section in the plastic hinge region and wrapped with composite straps.

MATERIALS

The materials used in the construction of specimens included: concrete with f'_c = 34.5 MPa (5000 psi) and Grade 40 steel rebars [nominal yield stress – 276 MPa (40 ksi)]. Although the specified concrete compression strength for the prototype bridge column was 21 MPa (3000 psi), ready-mixed concrete providing f'_c = 34.5 MPa (5000 psi) was used to include the effect of expected overstrength resulting from normal conservative mix design and strength gain with concrete aging. Table 1 summarizes the measured strength of concrete in all column specimens.

TABLE 1. Measured Concrete Compressive Strength.

Specimen	Age of Specimen at Testing (Days)	Average Compressive Strength of Three Cylinders (MPa)
R-1	245	34.9
R-2	260	35.7
R-3	165	33.3
R-4	235	35.6
R-5	240	36.2

All columns had a 240 x 368 mm (9.5 x 14.5 in.) rectangular cross section. Columns R-1 and R-2 were reinforced with 12 No. 5 Grade 40 longitudinal bars resulting in a reinforcement ratio of 2.7%. Columns R-3, R-4 and R-5 were reinforced with 10 No. 5 and 22 No. 4 Grade 40 longitudinal bars resulting in a reinforcement ratio of 5.45%. The transverse reinforcement for all five columns consisted of 9-gage steel wire ties, diameter 3.8 mm (0.148 in.), placed 89 mm (3.5 in.) on center along the entire height of the column. Table 2 summarizes the material properties of steel reinforcement.

TABLE 2. Material Properties of Steel Reinforcement.

Bar size	Grade	Average* Yield Stress (MPa)	Average* Yield Strain	Average* Hardening Strain	Average* Ultimate Strength (MPa)
No. 4	40	358	0.0021	0.0134	524
No. 5	40	359	0.0026	0.0146	556
9-gage wire	40	301	0.0036	**	**

* Based on three identical tests

** Data was not obtained

Composite straps with fiber volume ratio of 50.2% were used for all retrofitted specimens. The measured stress-strain relationship of this type of strap is shown in Figure 3. Other design details of the specimens are summarized in Table 3. Active and passive retrofit schemes refer to pressure in the gap between the strap and column face, or no pressure, respectively.

TABLE 3. Details of Column Specimens.

Specimen	Retrofit Scheme	Longitudinal Steel Detail	Longitudinal Steel Ratio	Confining Strap Configuration
R-1	Control (Not Retrofit)	Starter Bars	2.70%	None
R-2	Active	Starter Bars	2.70%	Rectangular
R-3	Control (Not Retrofit)	Continuous Bars	5.45%	None
R-4	Passive	Continuous Bars	5.45%	Rectangular
R-5	Passive	Continuous Bars	5.45%	Oval

TEST SETUP AND PROCEDURES

The setup was designed for testing column-footing assemblages subjected to lateral loading. The specimens were tested in a steel reaction frame as shown in Figure 7. Two independent loading systems were used to apply the load to the specimens. The axial load of 445 kN (100 kips) was applied to the column by prestressing a pair of 25 mm (1 in.) diameter high-strength steel rods against the base beams of the test frame, which was strongly bolted to the 915 mm (3 ft) thick concrete floor, before applying the lateral loads to the specimens. This load was applied to simulate the gravity load on the columns. The magnitude of this load was determined based on the scale factor of 1/5 over the tributary area resulting in a factor of 1/5 x 1/5 = 1/25. The prototype column had been designed for a gravity load of 0.15 $A_g f'_c$ or 11,200 kN (2500 kips), resulting in an axial load of 445 kN (100 kips) on the test columns. Lateral forces were generated by an HP-computer controlled MTS ± 489 kN (= 110 kips) hydraulic actuator mounted on the reaction frame. The actuator was capable of moving the top of the specimen 127 mm (5 in.) in both positive and negative directions. A displacement of 127 mm (5 in.) corresponds to a ratio of lateral displacement to column height of approximately 7%.

SIMULATED SEISMIC LOADING

The effect of an earthquake on the column specimen was simulated by reversed cyclic loading. The hydraulic actuator in the test setup was used to displace the top of the column to achieve a pre-determined load or displacement level. Then, the actuator was reversed to achieve the same load or displacement level in the opposite direction. The load and displacement input history was broken into two phases. At the initial stage, the test was in a load control mode. Upon yielding of the longitudinal rebars, a displacement control mode of loading was utilized. Figure 8 shows typical loading sequences of the columns. The letter "u" in this figure indicates the displacement ductility factor defined as the ratio of the applied displacement over the displacement at first yielding of the longitudinal rebars.

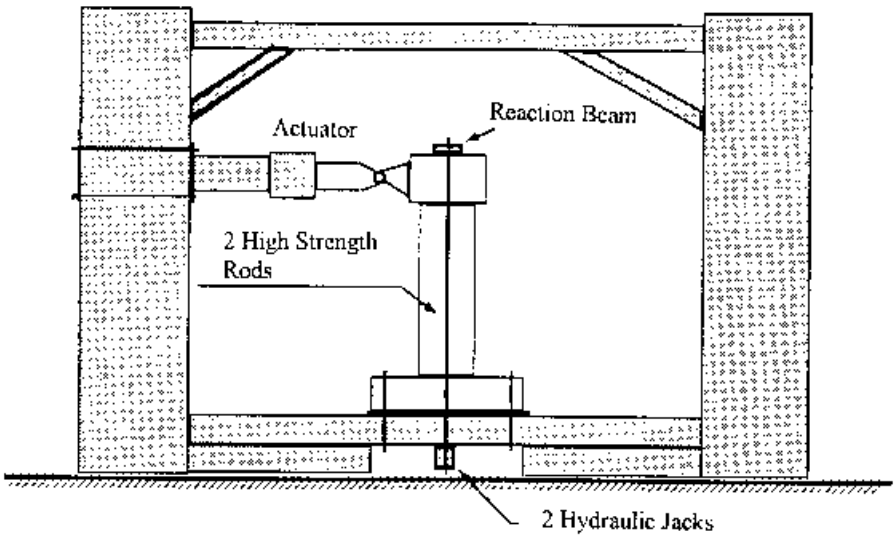

Figure 7. Test Setup.

LATERAL LOAD-DISPLACEMENT RESPONSE

The lateral load-displacement curves for all five specimens are shown in Figures 9 through 13. Because the columns were symmetrically reinforced with respect to the positive and the negative sides for each specimen, the resulting positive and negative portions of each specimen's hysteresis loops should be symmetrical and identical in values. However, due to the limitation of the hydraulic actuator, the maximum strokes reached by the actuator in the positive and negative directions were slightly different for some of the test specimens. The difference affected the symmetries of the hysteresis loops. In Figures 9 through 13, V_u is the lateral force corresponding to the theoretical flexural capacity of the unretrofitted column section, δ_y is the yield displacement which was used as a reference value to determine each subsequent displacement level that was applied to the specimen, and ρ_{sl} is the longitudinal reinforcement ratio of the column. The measured and calculated maximum strengths for the retrofitted and unretrofitted columns are summarized in Table 4. The calculated strength was determined using the procedures outlined in the ACI Code (ACI 1989) and taking into consideration the actual strain hardening properties of the reinforcing steel. The percent increase in strength was calculated with reference to the measured value for the control specimen.

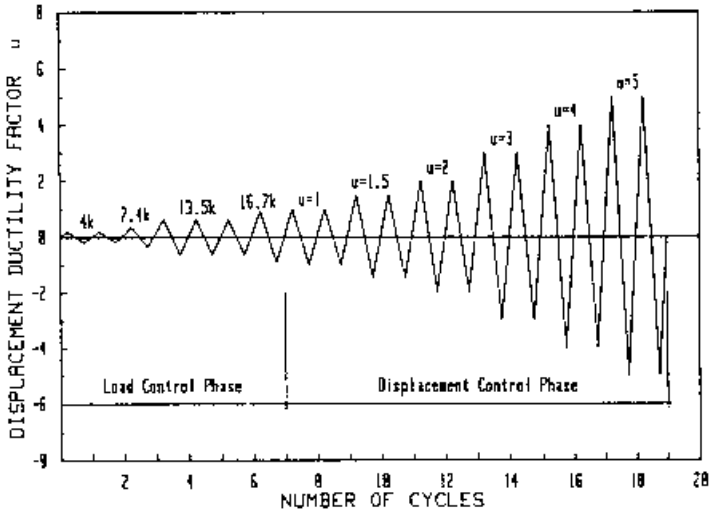

(a)

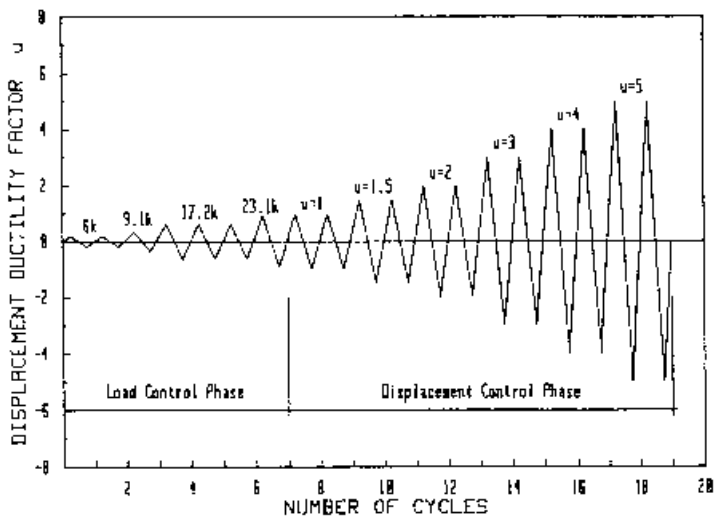

(b)

Figure 8. Loading sequence of test specimens; (a) columns with lapped starter bars and (b) columns with continuous reinforcement.

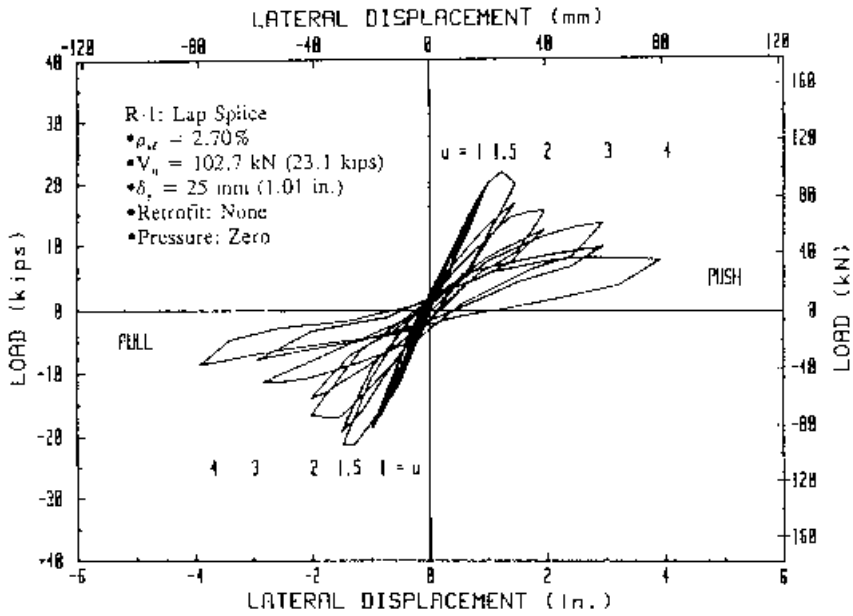

Figure 9. Load vs. displacement response of column R-1.

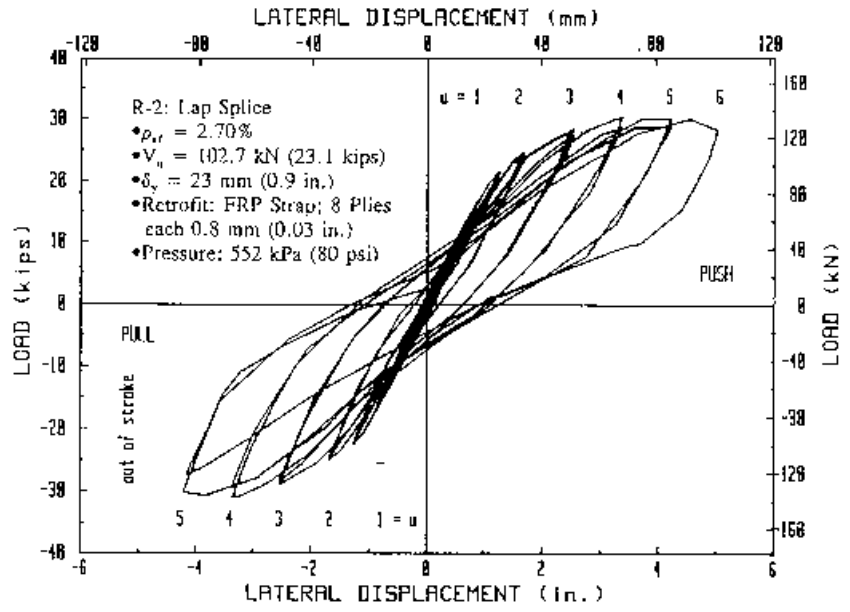

Figure 10. Load vs. displacement response of column R-2.

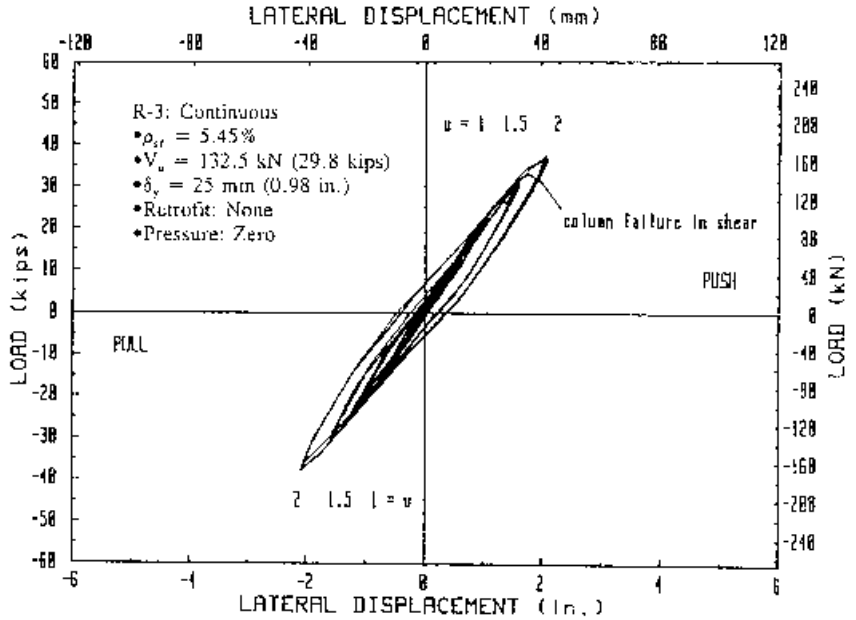

Figure 11. Load vs. displacement response of column R-3.

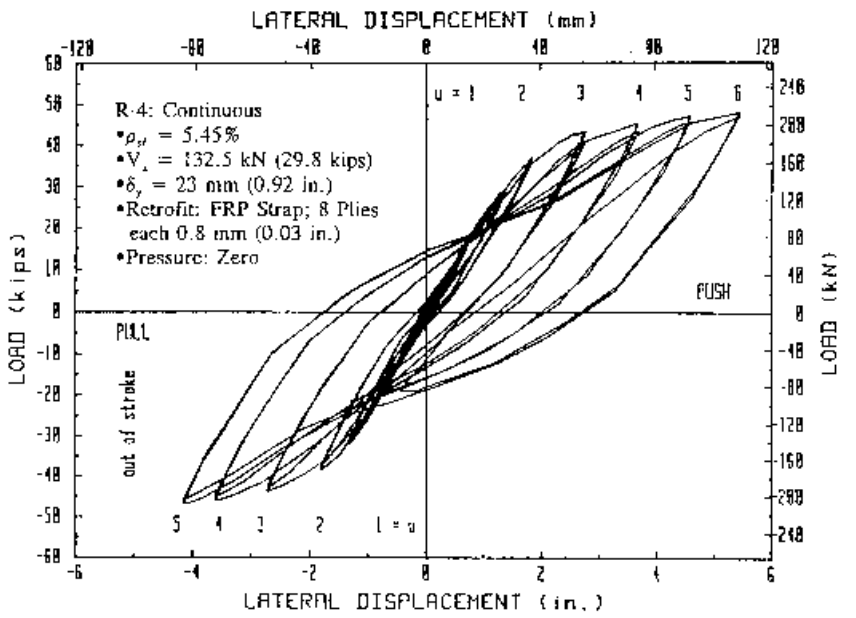

Figure 12. Load vs. displacement response of column R-4.

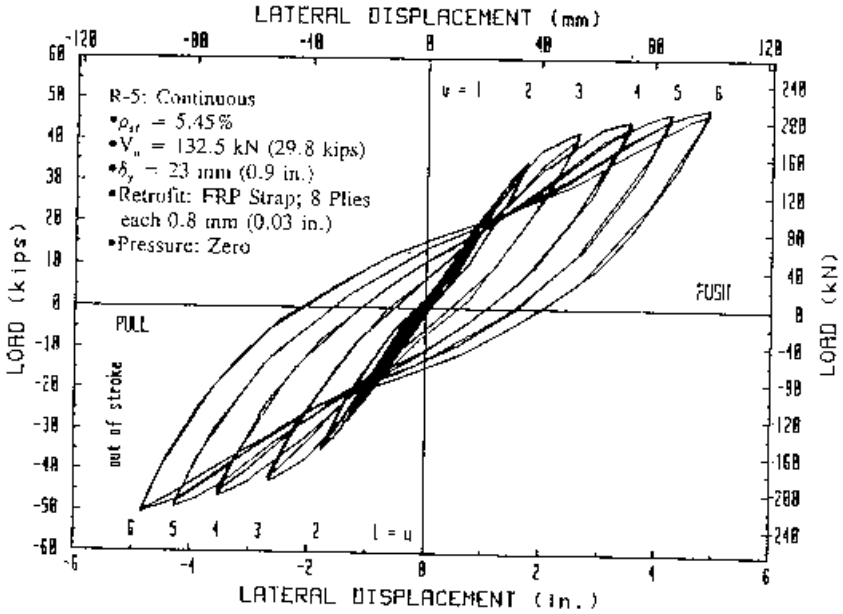

Figure 13. Load vs. displacement response of column R-5.

TABLE 4. Measured and Calculated Lateral Strength of Columns.

Specimens	Calculated Lateral Strength Using ACI (kN) (Unretrofitted)	Measured Maximum Lateral Load (kN) (Retrofitted)	Increase in Strength Resulting from Retrofitting
R-1	102.7	96.5	Control
R-2	102.7	138.8	44%
R-3	132.5	161.5	Control
R-4	132.5	214	32%
R-5	132.5	226.8	40%

The load-displacement curves of the two columns with lapped starter bars are shown in Figures 9 and 10. The hysteresis curves of the control specimen, R-1, shown in Figure 9, indicate that rapid degradation in strength occurred early and with very narrow energy dissipation loops. The lateral strength of column R-1 started to drop quickly at the first push cycle to u = 1.5. Because of bond failure in the lapped-spliced bars within the plastic hinge region of the column, the lateral load carrying capacity was reduced approximately by 80 percent of the calculated value at the ductility level of u = 4.

Column R-2 retrofitted with eight plies of FRP composite straps resulting in a total strap thickness of 6 mm (0.25 in.) and an active confinement scheme showed substantial improvement in the lateral load-displacement response as compared to column R-1, as shown in Figure 10. The presence of the confining strap prevented premature bond failure in the splice region. Consequently, the longitudinal bars could undergo significant plastic deformation, resulting in a larger lateral load and displacement capacities. It is noted, however, that the additional flexural capacity as a result of confinement with composite straps, could potentially lead to premature shear failure in the unwrapped portion of the column. If this is the case, the region outside the plastic hinge zone must be wrapped with adequate number of plies to develop the required shear capacity. The lateral load exceeded the predicted capacity of the unretrofitted column at the first cycle to u = 1.5. The column continued to resist more lateral loads up to the ductility level of u = ± 5 with very stable hysteresis loops. The maximum strength of 138.8 kN (31.2 kips) was recorded at the pull cycle of u = 5. A slight decrease in the column strength was noted at the ductility level of u = 6, which appeared to be due to small slippage between the main longitudinal reinforcement and the lapped starter bars.

The number of plies was calculated based on the required additional confinement pressure to bring the column to current design standards. During the initial stages of pressure injection, some of the epoxy would migrate up through the micro cracks and pores. Additional epoxy was injected to compensate for the loss of pressure due to this migration and to achieve a relative stable pressure at the desired level of 0.55 MPa (80 psi). It is anticipated that this pressure could further drop with time as this epoxy migration would continue. Moreover, this pressure could further drop as a result of the creep of epoxy and the wrap. However, at this low pressure level, the contribution of the latter two to the loss of pressure was expected to be minimal.

Figures 11 through 13 show the load vs. displacement responses of the three columns with continuous reinforcement and a higher longitudinal reinforcement ratio of 5.45 percent. Column R-3 was tested as the control specimen, and R-4 was retrofitted with rectangular shaped straps, while R-5 was retrofitted with oval shaped straps. It is believed that the oval-shaped composite straps are able to develop membrane confinement stresses, and hence, are expected to have better retrofit results, as compared with rectangular-shaped straps. Columns R-4 and R-5 were also wrapped with eight layers of composite strap. The load-displacement loops for column R-3 is shown in Figure 11. The predicted capacity of the column was reached at the displacement ductility level of u = 1.5. Some large flexural-shear cracks appeared within and beyond the plastic hinge zone at the ductility level of u = 2. On the way to the first push cycle to u = 3, extensive shear cracks along the whole height of the column were observed and longitudinal bars were suddenly separated from the core concrete due to the lack of adequate transverse reinforcement, resulting in a large drop of the lateral load carrying capacity. Figure 14 shows Column R-3 near failure.

Because column R-3 failed in shear, it was decided to strengthen columns R-4 and R-5 for both flexure and shear. In the plastic hinge region, these columns were wrapped with eight plies while the remaining portion of these columns were wrapped with only three plies.

Compared to R-3, the load-displacement responses of R-4 and R-5 were greatly improved, as shown in Figures 12 and 13, respectively. For both columns R-4 and R-5, stable hysteresis loops developed up to u = ± 6, and the measured lateral strength showed no sign of structural

degradation of the column. Unfortunately, the tests were terminated at a ductility level of u = 6, due to the limitation of the hydraulic actuator's stroke. The maximum increase in strength was measured at 214 kN (48.1 kips) for column R-4 and 224 kN (50.4 kips) for column R-5. The difference in the responses of the column with the rectangular shaped cross section and the column with the oval shaped cross section was not significant in this limited testing program. Additional tests must be conducted to establish the merits of modifying the cross section.

Figure 14. Shear cracks and failure of column R-3.

An examination of the hysteresis loops revealed that all specimens experienced some degree of pinching. More pinching in the loops were observed for the specimens with lapped starter bars than for the specimens with continuous reinforcement. Pinching is characterized by the narrow width of the hysteresis loops near mid-cycle, resulting in less energy dissipation per cycle as compared to a loop without pinching. Pinching is mainly caused by the slippage of the longitudinal bars and closing of flexural cracks in the plastic hinge zone of the columns.

LOAD VS. STRAIN

Figure 15 shows the location of various strain gages on the longitudinal reinforcements.

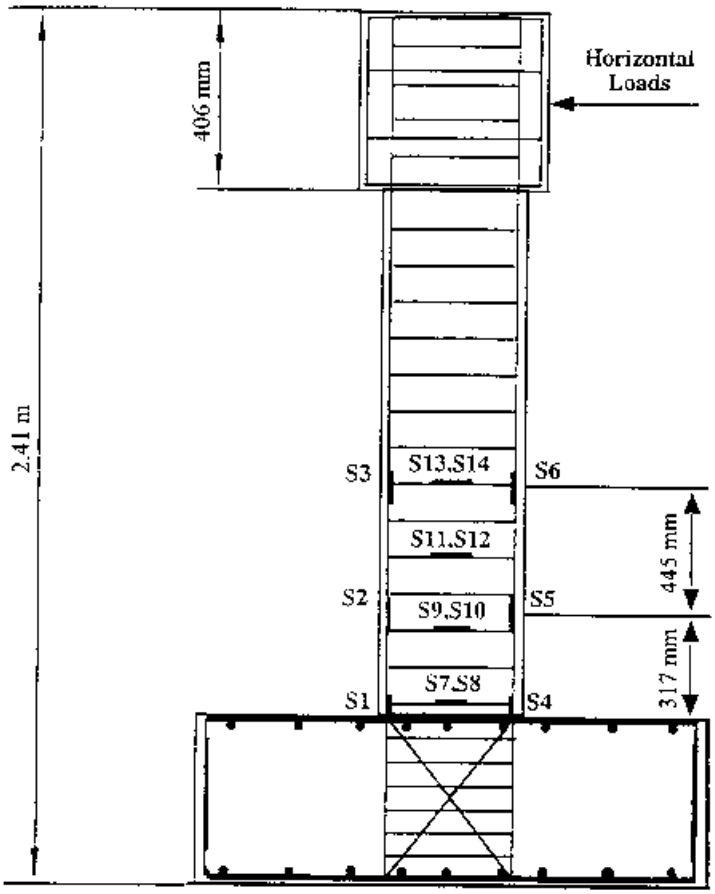

Figure 15. Locations of strain gages in columns.

The following describes strain measurements in different elements within the specimens

Longitudinal Reinforcement

Generally, the strains in the longitudinal reinforcements of the retrofitted columns were higher than those in the unretrofitted columns, indicating the effectiveness of the composite straps in confining the concrete and improving the bond, particularly at higher load levels. From the

longitudinal bar strains in this limited study, it was not possible to establish the merits of modifying the cross section. For example, there was not a clear difference between the strains of the longitudinal reinforcements in columns R-4 and R-5. Figures 16 and 17 show typical load vs. longitudinal bars strains at gage location S3 for columns R-4 and R-5, respectively. As can be seen from these figures, the strains were very close in both columns.

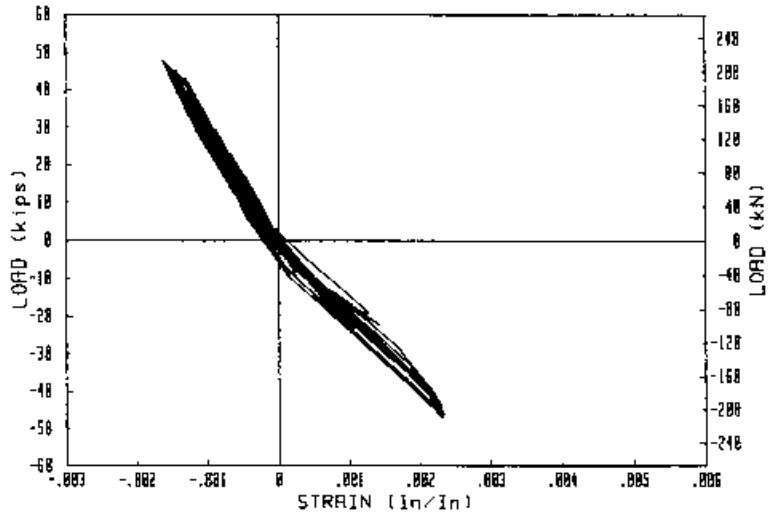

Figure 16. Load vs. strain in longitudinal bar of column R-4 at gage S3.

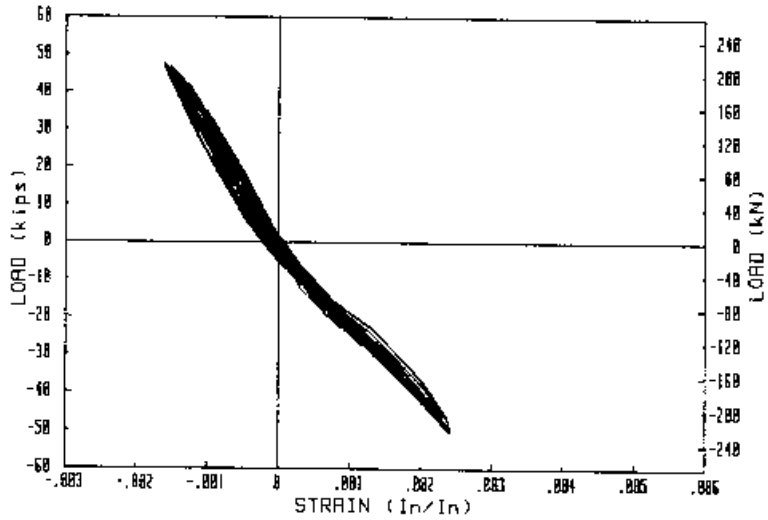

Figure 17. Load vs. strain in longitudinal bar of column R-5 at gage S3.

Transverse Reinforcement

The composite straps were very effective in confining the core concrete and sharing the hoop stresses as can be seen from typical load vs. hoop strains diagrams for unretrofitted and retrofitted columns shown in Figures 18 and 19. These figures show the load vs. strain at gage locations S11 and S12 for columns R-1 and R-2, respectively. Comparing these two figures shows that the strains in the hoop of the retrofitted column R-2 are smaller than the strains in the same hoop in the unretrofitted column R-1, even under higher lateral loads. This indicates that the confinement provided by the composite strap reduced the dialation of the core concrete in the retrofitted column, resulting in smaller hoop stresses in the transverse reinforcement.

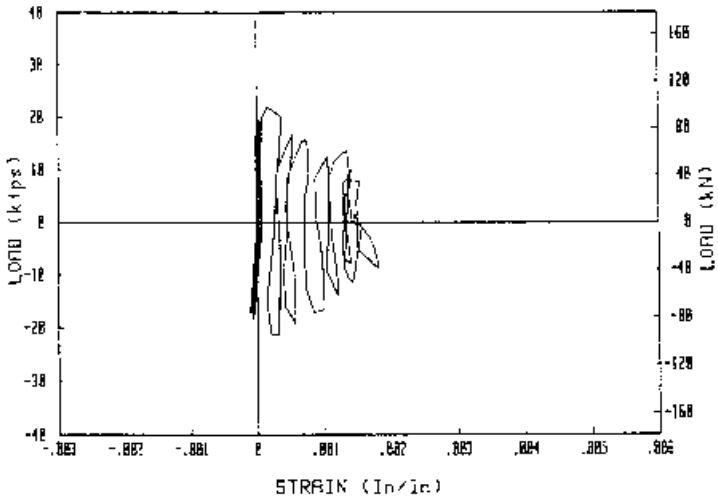

Figure 18. Load vs. strain in the hoop of column R-1 at gage S12.

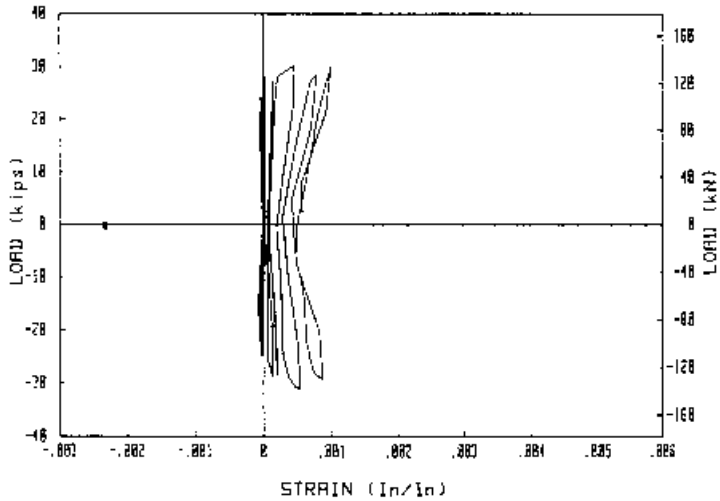

Figure 19. Load vs. strain in the hoop of column R-2 at gage S11.

Composite Strap

The effectiveness of the composite strap in confining the concrete core can also be verified through the column load or lateral displacement vs. strap strain. Figure 20 shows the lateral displacement at the top of the column R-2 vs. hoop strain in the strap at a location 318 mm (12.5 in.) above the top face of the footing. As can be seen from this figure, the strain in the strap increases successively with increasing lateral displacement, indicating the resistance developed in the strap to prevent the lateral expansion of the concrete core. Figures 21 and 22 show the lateral displacement at the top of the column vs. the hoop strain in the strap at the same location; that is, 318 mm (12.5 in.) above the top of the footing for columns R-4 and R-5, respectively. Comparing the maximum strains shown in those figures and the ultimate strap strain, it seems that the straps were over designed. The strap strain at a point closer to the top of the footing would be larger due to higher moment at that point. Furthermore, a high factor of safety must be used in the design of this system until such time when sufficient long-term field performance of this system has been observed and documented. The cross section of column R-5 was modified into an oval shape. The strain records in the composite strap for the two columns were too close to discern conclusively the effectiveness of this shape modification in improving the confining action of the straps.

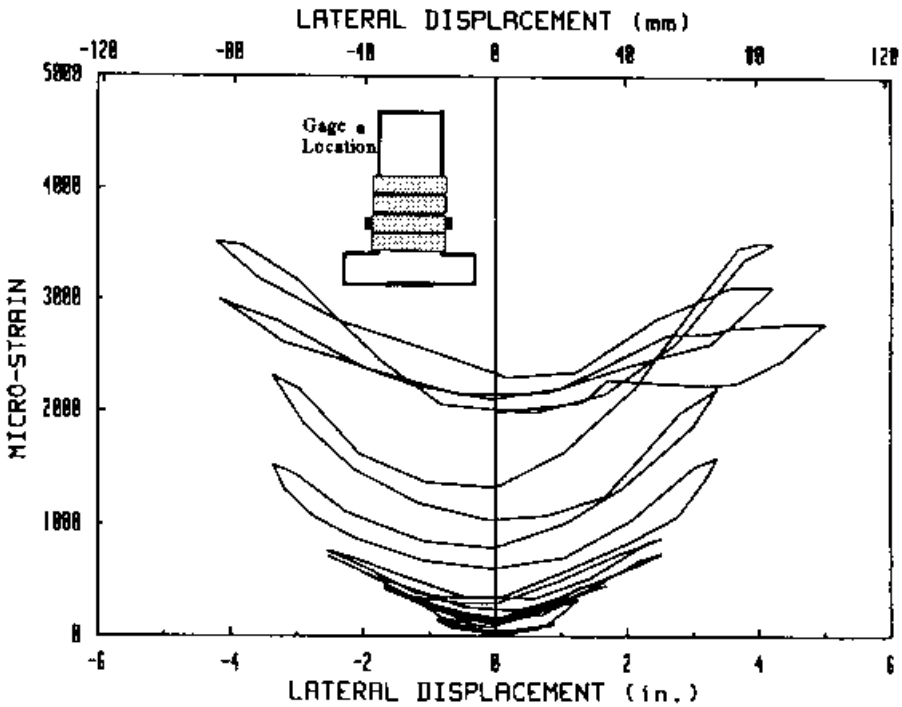

Figure 20. Deflection vs. average strap strain in column R-2 at gages SH3 & SH4.

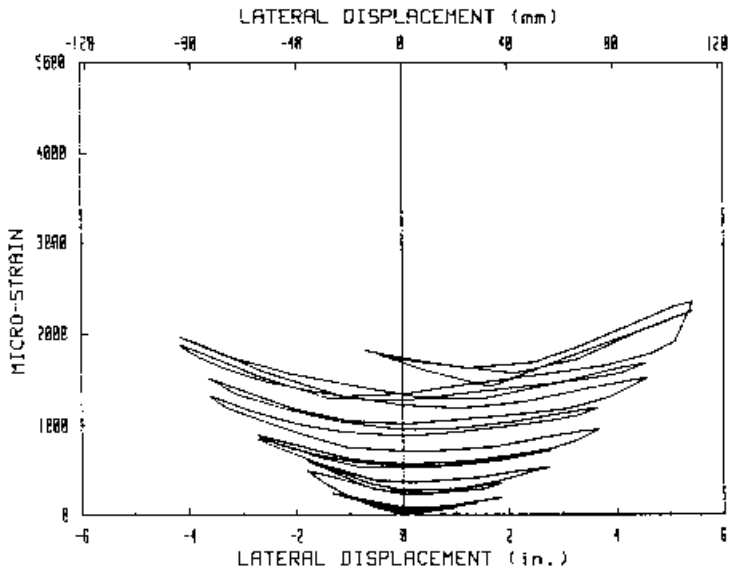

Figure 21. Deflection vs. average strap strain in column R-4 at gages SH3 & SH4.

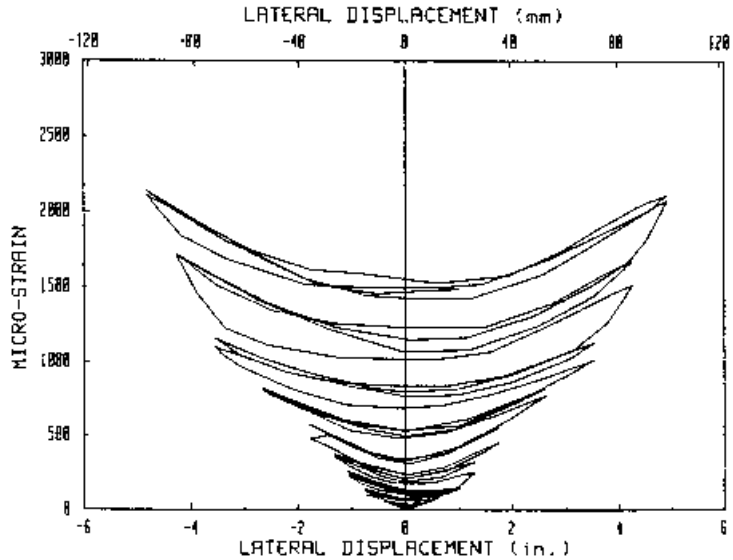

Figure 22. Deflection vs. average strap strain in column R-5 at gages SH3 & SH4.

COLUMN CRACKING AND FAILURE MECHANISM

Because all specimens for this study were designed with a strong footing detail, most of the cracking damage was concentrated in the column, especially within the plastic hinge region. For

the retrofitted columns, no major column cracking was observed during any of the load cycles. Two types of cracks, namely, flexural and shear, were observed during the test.

FLEXURAL CRACKS

In the unretrofitted columns, the flexural cracks spread from the bottom of the column up to about the mid-height of each specimen. The intervals of the flexural cracks were nearly the same as that of the transverse reinforcement spacing. The primary change of the behavior in R-1 occurred in the plastic hinge region of the column at the displacement ductility level of u = 1.5. At this stage of the test, the cover concrete spalled and the longitudinal reinforcement bars started to debond in the lapped-spliced region. As a result, lateral load-carrying capacity reduced rapidly at this displacement level. Subsequently, the column failed at the displacement ductility level of about u = 3, as a result of debonding of the longitudinal reinforcement in the lapped region, as shown in Figure 23. Column R-3, with the higher reinforcement ratio and continuous reinforcement, failed in shear at the displacement ductility level of u = 2.

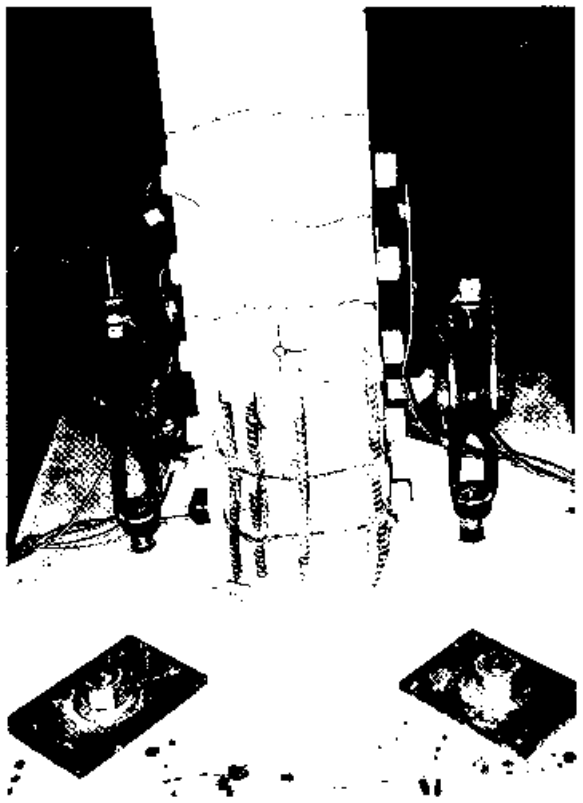

Figure 23. Debonding of longitudinal reinforcement.

SHEAR CRACKS

Large shear forces in column R-3, resulting from higher longitudinal reinforcement ratio of 5.45 percent, caused extensive diagonal shear cracks. Diagonal cracking has a marked effect on the failure mechanism of bridge columns, and can develop well outside the potential plastic hinge zone, particularly in columns with inadequate transverse reinforcement, as was shown for column R-3 in Figure 14. When the lateral load reached 147 kN (33 kips), the formation of diagonal shear cracks occurred at the mid-height of the column. At the push cycle of u = 2.0, corresponding to a lateral load of 160 kN (36 kips), the column longitudinal bars were suddenly separated from the core concrete, the lateral load dropped significantly, and the test was terminated.

CONCLUSIONS

The following conclusions are drawn based on the results of the limited tests conducted in this project, on non-ductile reinforced concrete columns strengthened by FRP composite straps:

1. Reinforced concrete bridge columns, designed before the new seismic design provisions were in place, and with lapped-spliced longitudinal reinforcement in the potential plastic hinge zone, appear to fail at low ductility levels of about 1.5. This is due to the debonding of the lapped starter bars, resulting from the lack of transverse reinforcement and insufficient development length of longitudinal bars. The failure modes are brittle because strength deterioration is very rapid following debonding of longitudinal reinforcement.

2. For rectangular columns designed with high longitudinal reinforcement ratio ($\rho_{sl} \approx 5\%$) and continuous reinforcement, brittle shear failure occurs due to insufficient transverse reinforcement. In this type of column, moment capacity is high resulting in high demand for shear capacity even at low ductility levels of u = 1.5.

3. Concrete columns externally wrapped with the FRP composite straps in the potential plastic hinge region showed a significant improvement in both strength and displacement ductility. The retrofitted columns developed very stable load-displacement hysteresis loops up to displacement ductility level of u = ± 6, without significant structural deterioration associated with the bond failure of lapped starter bars or longitudinal reinforcement buckling. The additional flexural strength may lead to potential premature failure in shear. In this case, shear strengthening of the column with composite wrap should also be considered. This was performed for columns R-4 and R-5, completely preventing shear failure of these specimens.

4. No major differences were observed in the test results between the oval-shaped straps and the rectangular-shaped straps within the range of the retrofit design parameters examined in this study. However, the results are not conclusive and additional studies must be undertaken to further investigate the behavior of rectangular columns retrofitted with oval-shaped composite straps.

ACKNOWLEDGEMENTS

The research reported in this paper was sponsored by the National Science Foundation (NSF) through grants MSS 9022667 and MS 9257344, Dr. John B. Scalzi, Program Director. The support of NSF is greatly appreciated. The experimental work was conducted in the Structural Laboratories of the University of Arizona. Assistance from the technical staff of the laboratories is gratefully acknowledged.

REFERENCES CITED

ACI Committee 318, "Building Code Requirements for Reinforced Concrete and Commentary (ACI 318M-89/ACI 318RM-89)," American Concrete Institute, 1989, 351 pp.

Katsumata, H., et al., "A Study with Carbon Fiber for Earthquake-Resistant Capacity of Existing Reinforced Concrete Column," Proceedings of the 9th Conference on Earthquake Engineering, Tokyo, Japan, Vol. 7, August 1988, pp. 517-522.

Priestly, M.J.N., Seible, F., and Anderson, Proof Test of a Retrofit Concept for the San Francisco Double-Deck Viaducts - Part 2: Test Details and Results," ACI Structural Journal, Vol. 90, No. 5, November-December 1993, pp. 616-631.

Priestly, M.J.N., Seible, F., Chai, Y.H., and Sun, Z., "Steel Jacketing of Bridge Columns for Enhanced Flexural Performance," Proceedings, NSF Symposium on Bridge Research in Progress, Des Moines, Iowa, 1988, pp. 205-208.

Sun, Z., Seible, F., and Priestly, M.J.N., "Diagnostics and Retrofit of Rectangular Bridge Columns for Seismic Loads," Proceedings of 8th U.S.-Japan Bridge Engineering Workshop, Chicago IL, 1992, pp. 282-296.